Journal of Applied Mechanics and Technical Physics, Vol. 36, No. 5, 1995

COMPLEX DEFORMATION OF AN ORTHOTROPIC MATERIAL

B. A. Rychkov

UDC 539.37

An attempt is made to describe the mechanism of deformation anisotropy of an orthotropic material under proportional and complex loadings in terms of the concept of sliding by means of generalization of the solid body model of [1, 2], which reflects a change in the strength properties of the material through a shear strength caused by slidings over the areas of basic tangential stresses.

1. Formulation of the Problem. At present, mostly variants of the plasticity theory of an orthotropic material with isotropic strengthening are being developed; one of these has been proposed by Hill [3] for sheet materials. This theory uses the Mises classical quadratic yield condition [4], which is in reasonably good agreement with experiments on loading along the orthotropy axes. However, this condition is "not easily adaptable in practice" [5]. For this reason, Hill began to develop its generalization using a uniform yield function of arbitrary (fractional) degree. Other generalizations of the yield condition, which take into account, for example, the influence of the first invariant of the stress tensor, are also available [6, 7].

The approach proposed in this work is based on experimentally observed different relations between components of the tensor of plastic deformation in its initial phase for different types of stresses. The case of biaxial tension where the basic directions of the stress tensor coincide with the symmetry axes of the initial anisotropy is considered.

Leonov et al. established [8], that under proportional loadings similar to uniaxial and biaxial tensions, an orthotropic material subjected to plastic defotmation first undergoes pure shear strain in one of the areas of basic tangential stresses. Consequently, if the shear mechanism of plastic deformation of polycrystals is taken as a basis, it is necessary to specify normal yield stresses (for example, the yield stress in uniaxial tension) by assigning them indices indicating the area and direction of sliding in it caused by the given stress. The averaged influence of basic tangential stresses on the process of sliding over a specific area can be taken into account by introducing an equivalent tangential stress [3], which is expressed in terms of the basic stresses:

$$\tau_{\text{equiv}}=\sqrt{\frac{1}{3(H_0+F_0+G_0)}\left[H_0(\sigma_z-\sigma_\varphi)^2+F_0(\sigma_\varphi-\sigma_r)^2+G_0(\sigma_r-\sigma_z)^2\right]}. \tag{1.1}$$

Here H_0, F_0, G_0 are the parameters of the initial anisotropy (at $H_0 = F_0 = G_0$ τ_{equiv} reduces to the octahedral tangential stress).

Assuming that the parameters H_0, F_0, and G_0 are determined by the yield stresses in three basic directions, we suggest that the yield condition in the plane be taken in the form

$$\tau_{ij} = B_{ij} - k\tau_{\text{equiv}}, \qquad B_{ij},\ k = \text{const} \quad (i,j = z,\varphi,r), \tag{1.2}$$

where τ_{ij} are the yield stresses in the areas of basic tangential stresses; B_{ij}, k are the material parameters; the indices z, φ, and r show the direction along the tube axis tangential to its generatrix and along the tube radius, respectively, for tension with internal pressure of a thin-walled tube (the main case of loading considered herein).

The model of strengthening of an orthotropic material discussed below is primarily related to the properties of zirconium alloy E-110. Its yield stress of axial tension [8] is $(\sigma_z^{\gamma})_{z\varphi} \approx 10 \cdot 9.81$ MPa (the second

Institute of Automation, Academy of Sciences of the Kirghis Republic, Bishkek 720075. Translated from Prikladnaya Mekhanika i Tekhnicheskaya Fizika, Vol. 36, No. 5, pp. 87–97, September–October, 1995. Original article submitted November 3, 1993; revision submitted October 11, 1994.

0021-8944/95/3605-0715 $12.50

index z, φ in the notation of the yield stress indicates the area of basic tangential stress, over which the first slidings occur). In tension in the transverse direction, $(\sigma_\varphi^y)_{\varphi z} \approx 32 \cdot 9.81$ MPa (at a 0.1% tolerance for the largest basic deformation). Even these two yield stresses give an indication of significant initial anisotropy. It is reflected by condition (1.2) as follows.

Taking the yield stress for $k_\sigma = 4/3$ ($k_\sigma = \sigma_z/\sigma_\varphi$), which is the stress σ_z, as the initial data (along with the indicated uniaxial stresses), and taking into account that for this stressed state (as in the case $k_\sigma = \infty$) the initial values of the plastic deformation components also satisfy the relation

$$\Gamma_z \approx -\Gamma_\varphi, \tag{1.3}$$

we find that at the tolerance taken for Γ_z

$$(\sigma_z^y)_{z\varphi} \approx 14.8 \cdot 9.81 \text{ MPa} \quad \text{at} \quad k_\sigma = 4/3. \tag{1.4}$$

Using the yield stresses at $k_\sigma = \infty$ and 4/3, in view of (1.2), we obtain

$$k = 1.4, \qquad B_{z\varphi} = 13.16 \cdot 9.81 \text{ MPa}. \tag{1.5}$$

In contrast to the basic tangential stresses τ_{ij}, the "areas of sliding" will be denoted by T_{ij}, as in the model of an initially-isotropic material [9]. From the axial tension diagram for the material being considered it follows that the area $T_{z\varphi}$ is "brought into action" after the area T_{zr} at tension $\sigma_z \approx 16.5 \cdot 9.81$ MPa, i.e., the yield stress $(\sigma_z^y)_{zr}$ for $k_\sigma = \infty$ is equal to the indicated value. This makes it possible to compute the constant B_{zr} by using the value parameter k (1.5):

$$B_{zr} = 21.72 \cdot 9.81 \text{ MPa}.$$

The calculations, in accordance with condition (1.2), showed that, for the parameters of the material found in this way, slidings occur simultaneously over the areas $T_{z\varphi}$ and T_{zr} at a stress close to equal biaxial tension ($k_\sigma = 0.986$). Indeed, a deviation from equality (1.3) such that $\Gamma_z > |\Gamma_\varphi|$ is observed in the experiment for this case in the small vicinity of the conditional yield stress.

The other parameters of the material model introduced and the corresponding yield stresses over the slidings areas at different stresses are determined in a similar manner. The calculated data and the corresponding experimental data confirm that the yield condition (1.2) for the value (1.5) of the parameter k is suitable for the zirconium alloy. Its distinctive feature is an increase in the biaxial strength in comparison to uniaxial tension. This phenomenon was observed, for example, for a titanium alloy in [10].

It turned out that, for $0 \leqslant k_\sigma \leqslant \infty$, the yield stresses of the titanium alloy [10] correspond to condition (1.2) if the area $T_{z\varphi}$ is "working" for $\infty \geqslant k_\sigma \geqslant 1.014$ and the area $T_{\varphi z}$ is working for $1.014 \geqslant k_\sigma \geqslant 0$. The yield stresses $(\sigma_\varphi^y)_{\varphi z} = 87.2 \cdot 9.81$ MPa ($k_\sigma = 0$), $(\sigma_z^y)_{z\varphi} = 90.7 \cdot 9.81$ MPa ($k_\sigma = \infty$), $(\sigma_\varphi^y)_{\varphi z} = 112.5 \cdot 9.81$ MPa ($k_\sigma = 0.5$) were used as initial data for determining the material parameters (k, $B_{z\varphi}$, and $B_{\varphi z}$). The calculated yield curve is shown in Fig. 1 by a solid line, and the experimental data, by a dotted line. The dashed and dash-dotted lines represent the yield curves constructed [10] by using the Hill theory (and the Mises–Hill corresponding yield condition) with the following assumptions.

Transverse isotropy of the material [10] is assumed, and the relation between the increments of the deformation components at axial tension, $d\varepsilon_\varphi/d\varepsilon_r = R$, is used for determining the parameters of the initial anisotropy. The dashed line is constructed from the initial yield stresses for $k_\sigma = 0$ and 0.5 at $R = 1.7$, and the dash-dotted line from of the data for $k_\sigma = 0$ and 1 at $R = 2.6$.

Thus, also for the titanium alloy, yield condition (1.2) agrees with experimental data better than the Mises–Hill condition.

It should be noted that the Mises–Hill yield condition for a transversally isotropic material in the case of biaxial stress is transformed (at $H_0 = G_0$) into the form

$$F(\sigma_z, \sigma_\varphi) = 2H_0(\sigma_z - \sigma_\varphi)\sigma_z + (H_0 + F_0)\sigma_\varphi^2 = 1.$$

The yield condition below, which is similar to condition (1.2) and is "intermediate" between the criteria of

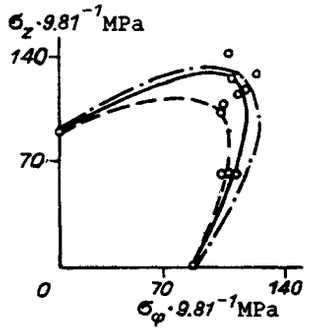

Fig. 1

Mises–Hill and of Tresca, was proposed [11] for such a material:

$$\eta\Sigma + (1-\eta)t_{nl} = 1 \qquad (0 \leqslant \eta \leqslant 1). \tag{1.6}$$

Here η is a material parameter determined from the experiment;

$$\Sigma = \sqrt{F(\sigma_z, \sigma_\varphi)}; \qquad t_{nl} = \frac{|\sigma_k - \sigma_l|}{\sigma_k^y} \quad (k = 1,2,\ l = 2,3,\ k \neq l).$$

A comparison of expressions (1.2) and (1.6) shows that the latter imposes a more severe limitation on the coefficients of the linear dependence between the basic tangential stresses and the equivalent stress. Condition (1.6) gives practically the same result as condition (1.2) only for materials with insignificant initial anisotropy and a slight increase in biaxial strength (for example, for aluminum alloy D16T [12] and magnesium alloy MA2 [13]). Condition (1.6) is not satisfactory for zirconium and titanium alloys, as is clear from the determination of the parameter η in the light of the previous analysis.

2. Shear Strength. Plastic Strain Tensor. The left-hand side of equality (1.2) is, in essence, the initial shear strength, i.e., the local yield stress in a given plane in a specified direction. With increase in the stress level, which will be characterized by the equivalent tangential stress (1.1), the shear strength increases due to increase in the intensity of slidings. It is believed that the shear strength S_{il} in each of the sliding areas T_{ij} depends directly only on the intensity of slidings r_{il} over this area, as was assumed in the simplified concept of sliding in [1, 2]. We shall assume that

$$S_{il} = \psi(\tau_{\text{equiv}}, \tau_{ij}) + \Psi(\tau_{\text{equiv}}, \tau_{ij}) r_{il} + A_{ij}(1 - \cos \widehat{jl}), \quad A_{ij} = \text{const} \tag{2.1}$$

for the case of loading with invariable basic directions. Here the direction l in the plane T_{ij} is measured from the direction j of the corresponding basic tangential stress. The function of influence of elastic strains ψ is expressed by analogy with an isotropic case [2]:

$$\psi(\tau_{\text{equiv}}, \tau_{ij}) = [B_{ij} - (k - \Pi_{ij}\tau_{ij}/\tau_{\text{equiv}})\tau_{\text{equiv}}]/(1 + \Pi_{ij}).$$

In this function, the parameter Π_{ij} regulates its variation taking into account the fact that a quick (or slow) decrease in the function ψ under monotonic loading leads, respectively, to quick (slow) growth of the fan of slidings. The activity of the sliding areas for the zirconium alloy turned out to be different; on the basis of the data of proportional loading for the basic acting areas T_{ij}, it can be assumed that

$$\Pi_{z\varphi} = 0, \qquad \Pi_{zr} = 3(1 - \tau_{z\varphi}/\tau_{zr}), \qquad \Pi_{\varphi z} = 0, \quad \Pi_{\varphi r} = 4(1 - \tau_{\varphi z}/\tau_{\varphi r}) k_\sigma^{1.1} \cos(2\pi k_\sigma).$$

The parameter Π_{ij} does not influence the initial yield condition: the equality $S_{ij}|_{\tau_{ij} \equiv 0} = \tau_{ij}$ leads to relation (1.2).

The third term in expression (2.1) shows how much the shear strength would increase with distance from the direction of the basic tangential stress; together with the first term, it influences the span of the fan

of slidings. The values of the parameters A_{ij} are taken equal to the doubled normal yield stress which causes slidings over the corresponding area T_{ij}.

The function $\Psi(\tau_{\text{equiv}}, \tau_{ij})$ determines the type of the material strengthening, being a sort of an analog of the cutting modulus. It is convenient to take the difference $\tau_{ij} - \psi(\tau_{\text{equiv}}, \tau_{ij})$ as its argument, which gives

$$\Psi(\tau_{\text{equiv}}, \tau_{ij}) = p_{ij}\left[\frac{\tau_{ij} + k\tau_{\text{equiv}}}{B_{ij}} - 1\right]^{c_{ij}}, \qquad p_{ij},\ c_{ij} = \text{const}.$$

After determining the direction of sliding over the areas T_{ij} by the angle β, using the rule given above, we find the intensity of slidings $r(\beta) \equiv r_{il(\beta)}$ from the condition of equality of the shear strength to the corresponding tangential stress. Summing the elementary shears over individual areas T_{nl}, we determine the constituents of the plastic strain tensor components in the basic axes (i, j):

$$(\Gamma_i)_{nl} = -(\Gamma_j)_{nl} = \frac{1}{2}\int_{-\theta_{ij}}^{\theta_{ij}} r(\beta)\cos 2\beta\, d\beta \quad (i, j = z, \varphi, r). \tag{2.2}$$

Here the indices n, l indicate the area over which slidings at a specific level and type of stress occur, i.e., n and l also "run through" the basic directions.

Adding up components (2.2), we obtain the sought-for deformations:

$$\Gamma_i = \sum_{n,l}^{i,j}(\Gamma_i)_{nl} \qquad (i = z, \varphi, r), \tag{2.3}$$

with allowance for the condition of plastic incompressibility.

The boundaries of the fan of slidings $\pm\theta_{ij}$ are determined from the continuity condition for sliding, i.e., from the condition $r(\pm\theta_{ij}) = 0$, which gives

$$\cos 2\theta_{ij} = [\psi(\tau_{\text{equiv}}, \tau_{ij}) + A_{ij}]/(\tau_{ij} + A_{ij}). \tag{2.4}$$

Thus, formulas (2.2)–(2.4) relate the given stresses to the components of the plastic strain tensor. This relation includes, in addition to the material parameters described above, the constants p_{ij} and c_{ij}. They are found by approximating the initial strengthening diagrams, for which we take the axial tension diagram and those diagrams of proportional loading which show, by variation of the strain components, when each of the sliding areas T_{ij} is first brought into action.

3. Loading Trajectory Excluding the Baushinger Effect. Let us consider a two-link loading trajectory in the space of tensions $\sigma_z \sim \sigma_\varphi$, the first link of which is uniaxial tension. Let us change the slope of the second link of the trajectory in order to avoid difficulties caused by the Baushinger effect in the computation of the components of the plastic strain tensor in orthogonal additional loading [8]. The Baushinger effect will be absent if it is required that during subsequent additional loading no unloading would appear in any of the directions of slidings occurring under tension. It is clear from the previous discussion that in this particular case the area $T_{z\varphi}$ is meant. This requirement will be satisfied if the intensity of slidings $r_{z\varphi}$ in the direction of the basic tangential stress $\tau_{z\varphi}$ will not decrease, i.e., if the equality

$$\dot{\psi}(\tau_{\text{equiv}}, \tau_{z\varphi}) + \Psi(\tau_{\text{equiv}}, \tau_{z\varphi})r^*_{z\varphi} = \tau_{z\varphi} \tag{3.1}$$

will always be valid in loading on the second link, where $r^*_{z\varphi}$ is the intensity of slidings in the indicated direction at the moment of additional loading.

Removing the parenthesis in the left-hand side of equality (3.1), after some transformations we obtain the relation between the current stresses and their values at the moment of additional loading:

$$\tau_{z\varphi} + k\tau_{\text{equiv}} = \tau^*_{z\varphi} + k\tau^*_{\text{equiv}}. \tag{3.2}$$

This equation is the equation of a small curvature line in the space $\sigma_z \sim \sigma_\varphi$. In loading along this curve, the intensity r_{zl} ($l \in [-\theta_{z\varphi}, \theta_{z\varphi}]$) increases in directions different from the direction φ (mean direction in the area of slidings), while the value of $r_{z\varphi}$ remains constant (equal to $r^*_{z\varphi}$). However, in comparison with the previous

TABLE 1

Reference point number in the experiment	$\sigma_z \cdot 9.81$	$\sigma_\varphi \cdot 9.81$	ε_z	$-\varepsilon_\varphi$
	MPa		%	
1	10.63	0	0.17	0.08
2	17.34	0	0.31	0.19
3	22.48	0	0.49	0.30
4	23.79	0	0.60	0.38
5	26.20	0	0.96	0.50
6	27.90	0	1.28	0.72
7	28.75	1.90	1.47	0.87
8	32.35	9.91	1.71	0.93
9	34.90	15.90	1.79	0.93
10	31.45	7.95	1.83	1.00
11	27.90	0	1.94	1.16
12	30.37	0	2.05	1.22
13	31.39	0	2.18	1.36
14	34.93	0	2.90	2.58
15	36.86	0	4.10	3.67

tension, the area of slidings increases only slightly right up to the critical tension σ_z^{cr} but begins to expand quickly as this critical stress is exceeded. As the tension σ_z is varied from σ_z^* to σ_z^{cr}, the curve (3.2) can be replaced by a straight line with no changes in this peculiarity of propagation of slidings. The second link of the loading trajectory was given in just this way. In motion along this link, the Baushinger effect should be absent (in accordance with the model), and the increments of the plastic strain tensor components due to the slidings over the area $T_{z\varphi}$ should be small. It is easy to verify that the slidings over the area T_{zr} (if it has already acted, together with the area $T_{z\varphi}$, in axial tension) will cease. This means that the revealed additional loading causes an increase in pure shear strain, a factor that should be confirmed or rejected by experiment.

The experiments were carried out at $\sigma_z^* = 28 \cdot 9.81$ MPa, $\Delta\sigma_z/\sigma_\varphi = 0.44$ $(\sigma_z = \sigma_z^* + \Delta\sigma_z)$, $\sigma_z^{cr} = 35 \cdot 9.81$ MPa. After realization of such a two-link loading trajectory, unloading to the corner point of the trajectory was accomplished, followed by repeated loading along rays coming from this point, at the ratio $\Delta\sigma_z/\sigma_\varphi \leq 0.44$. The initial experimental data of five samples tested are given (as is strongly recommended in [14]), respectively, in the form of Tables 1–5, which were put at our disposal by V. M. Zhigalkin and which supplement the previous experiments with zirconium alloy E-110.

Before comparing the calculated and experimental data, we should note the following fact. In accordance with the model, initial loading along the two-link trajectory specified in this way causes monotonic deformation, i.e., in any of the directions of slidings their intensity does not decrease, and the Baushinger effect does not manifest itself (the two phenomena are interrelated). Therefore, the strengthening diagrams obtained after unloading into the corner point of the trajectory in repeated loading should tend to similar diagrams for proportional loading, provided that the stressed states in the both cases are of the same type. The results of proportional and complex loading are grouped (in samples) with allowance for this expected behavior of the material and are presented in Figs. 2 and 3. The trajectories of proportional loading are characterized by the ratio $k_\sigma = \sigma_z/\sigma_\varphi$ and the trajectories of complex loading, by $k_{\Delta\sigma} = \Delta\sigma_z/\sigma_\varphi$. The calculated diagrams $\sigma_z(\varepsilon_z)$ and $\sigma_\varphi(\varepsilon_\varphi)$ are shown in Figs. 2 and 3 by dashed lines (first case), solid lines (second case), and dotted lines (experimental data).

The common peculiarity in the behavior of the material in the initial section of the second link of the trajectory is as follows: in the initial additional loading the increment rates of the strain components ε_z and ε_φ, which took place at the earlier moment of axial tension, remain almost unchanged. This is apparently due to the lag of the vector properties of the strains. In this case, as with isotropic materials, the lag trace,

TABLE 2

Reference point number in the experiment	$\sigma_z \cdot 9.81$	$\sigma_\varphi \cdot 9.81$	ε_z	$-\varepsilon_\varphi$
	MPa		%	
1	12.40	0	0.14	0.06
2	18.22	0	0.29	0.13
3	20.75	0	0.39	0.20
4	22.78	0	0.61	0.30
5	24.55	0	1.05	0.64
6	27.90	0	1.79	1.22
7	29.20	2.90	2.00	1.37
8	34.90	15.90	2.16	1.43
9	27.90	0	2.28	1.56
10	29.10	0.58	2.35	1.64
11	30.16	1.21	2.48	1.80
12	34.23	3.53	2.95	2.58
13	36.35	4.46	3.62	3.09
14	37.70	5.04	5.20	3.80
15	50.00	6.72	9.53	5.20

TABLE 3

Reference point number in the experiment	$\sigma_z \cdot 9.81$	$\sigma_\varphi \cdot 9.81$	ε_z	$-\varepsilon_\varphi$
	MPa		%	
1	13.41	0	0.17	0.03
2	21.50	0	0.46	0.16
3	24.20	0	0.75	0.35
4	27.90	0	1.40	0.75
5	29.60	3.94	1.90	1.04
6	30.90	7.00	1.98	1.08
7	33.50	11.94	1.99	1.08
8	34.90	15.90	2.05	1.08
9	27.90	0	2.23	1.33
10	30.40	2.50	2.48	1.52
11	35.40	7.50	2.69	1.70
12	36.30	8.46	2.80	1.82
13	40.50	12.64	3.40	2.58
14	43.00	16.12	4.12	3.84
15	45.46	17.57	4.46	4.27

TABLE 4

Reference point number in the experiment	$\sigma_z \cdot 9.81$	$\sigma_\varphi \cdot 9.81$	ε_z	$-\varepsilon_\varphi$
	MPa		%	
1	19.24	0	0,21	0.08
2	22.78	0	0.29	0.15
3	23.84	0	0.46	0.28
4	25.44	0	0.70	0.63
5	27.90	0	1.18	1.17
6	30.10	5.00	1.34	1.34
7	34.90	15.90	1.37	1.34
8	27.90	0	1.40	1.48
9	36.50	27.26	1.47	1.38
10	37.94	32.13	1.50	1.35
11	40.29	38.51	1.55	1.24
12	41.25	41.76	1.62	1.13
13	41.71	43.78	1.65	1.02
14	42.80	46.57	1.78	0.64
15	43.27	48.10	1.96	0.18

TABLE 5

Reference point number in the experiment	$\sigma_z \cdot 9.81$	$\sigma_\varphi \cdot 9.81$	ε_z	ε_φ
	MPa		%	
1	16.70	0	0.24	−0.10
2	20.50	0	0.37	−0.16
3	22.27	0	0.58	−0.26
4	27.90	0	1.19	−0.63
5	29.27	3.12	1.54	−0.84
6	34.90	15.90	1.69	−0.84
7	27.90	0	1.76	−0.95
8	31.70	21.57	1.75	−0.90
9	33.17	31.08	1.75	−0.72
10	35.45	38.51	1.76	−0.50
11	35.45	43.26	1.77	−0.20
12	36.68	48.10	1.78	0.84

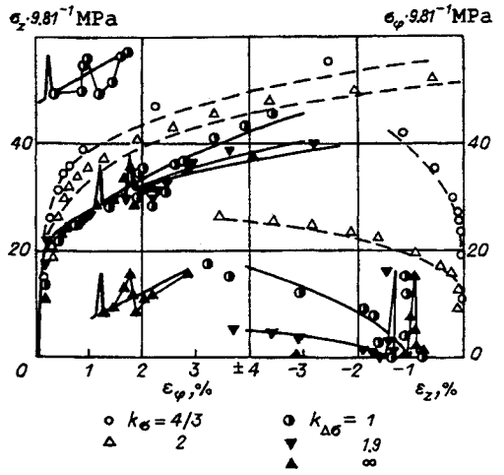

Fig. 2

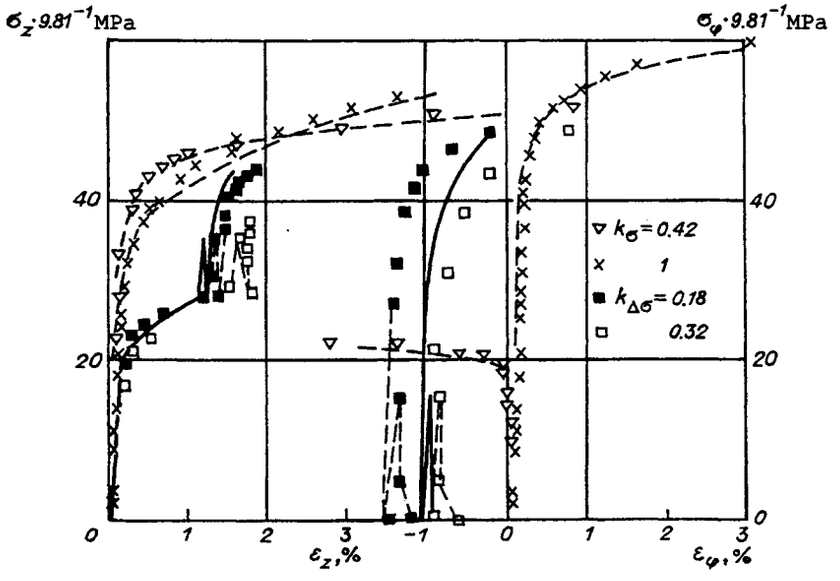

Fig. 3

measured by the length of the second link, is approximately 1/10th of the length of the first link of the tensions' trajectory. If the lag trace is not taken into account, the calculated and experimental diagrams $\sigma_z(\varepsilon_z)$ and $\sigma_\varphi(\varepsilon_\varphi)$ are similar.

Thus, a pure shear strain ($\Delta\Gamma_z = |\Delta\Gamma_\varphi|$) predicted by the material model proposed for the two-link loading trajectory (at a specific angle of deflection) actually takes place in the second link of the trajectory, but with some displacement due to the lag property, and with a natural deviation from the equality $\Delta\Gamma_z = |\Delta\Gamma_\varphi|$ in both directions. In repeated ("radial") loading, the predictions of the model were also confirmed: the strengthening diagrams for each "ray" tended to similar diagrams for proportional loading, with the same type of stressed state in both cases.

It should be noted that, for four samples, the coefficient k_{red} [9] for reducing the strengthening diagram to the nominal diagram for this material could be taken equal to unity; only for $k_{\Delta\sigma} = 1.9$ is $k_{\text{red}} = 1.05$. Therefore, it is necessary to increase the experimental values of tensions by a factor of 1.05, so that the calculated and observed strengthening diagrams can be compared. The corner point of the loading trajectory for this sample is appropriately shifted and this is reflected in Fig. 2 as the second "peak" in the calculated

diagrams $\sigma_z(\varepsilon_z)$ and $\sigma_\varphi(\varepsilon_\varphi)$ corresponding to the second law.

The general conclusion from the results of complex loading is as follows: if the strained state of the material under preliminary loading is formed due to slidings over two areas T_{ij}, then, with a change of the stressed state and an increase in the level of stresses, the slidings continue only over one of these areas or occur in a third similar area. This leads to a vastly greater strengthening of the material in comparison to that in preliminary loading. This strengthening effect can be controlled, as shown by the experiments conducted, by means of the orthotropic material model whose basic strength characteristic is shear strength.

REFERENCES

1. M. Ya. Leonov, E. B. Nisnevich, and B. A. Rychkov, "Plane theory of plasticity based on the synthesis of slidings," *Izv. Akad. Nauk SSSR, Mekh. Tverd. Tela*, No. 6, 43–49 (1979).
2. B. A. Rychkov, "Complex deformation of plastic materials in loadings without rotation of the basic axes of the stress tensor," *Izv. Ross. Akad. Nauk, Mekh. Tverd. Tela*, No. 1, 112–119 (1993).
3. R. Hill, *Mathematical Theory of Plasticity* [Russian translation], Gostekhteoretizdat, Moscow (1956).
4. R. Mises, "Mechanic der plastischen Formanderung von Kristallen," *Z. Angew. Math. Mech.*, **8**. H. 3 (1928).
5. R. Hill, "Constitutive modelling of orthotropic plasticity in sheet metals," *J. Mech. Phys. Solids*, **38**, No. 3, 405–417 (1990).
6. V. V. Kosarchuk, B. I. Kovalchuk, and A. A. Lebedev, "Experimental investigation of the strengthening laws of initially anisotropic materials," *Probl. Prochnosti*, No. 9, 3–9 (1982).
7. M. A. Grekov, "Plasticity of an anisotropic body," *Dokl. Akad. Nauk SSSR*, **278**, No. 5, 1082–1085 (1984).
8. V. M. Zhigalkin and B. A. Rychkov, "Anisotropic strengthening of an orthotropic material." *Prikl. Mekh. Tekh. Fiz.*, **36**, No. 5, 81–86 (1995).
9. V. M. Zhigalkin and B. A. Rychkov, "Anisotropy caused by slidings," *Prikl. Mekh. Tekh. Fiz.*, **35**, No. 3, 136–144 (1994).
10. Kh. V. Babel', D. A. Atman, and R. V. Makiver, "Biaxial strengthening of anisotropic titanium alloys," *Proc. of Am. Soc. Mech. Eng. Theor. Foundation of Eng. Calculations*: Transl. J. *Trans. ASME. J. Basic. Eng.*, **89**, No. 1, 15–23 (1967).
11. A. A. Lebedev, V. V. Kosarchuk, and B. I. Kovalchuk, "Investigation of the scalar and vector properties of anisotropic materials in a complex stressed state. Communication 1. On the yield condition of anisotropic materials," *Probl. Prochnosti*, No. 3, 25–31 (1982).
12. A. M. Zhukov, "Strength and plasticity of D16T alloy in a complex stressed state," *Izv. Akad. Nauk SSSR*, No. 6, 61–70 (1954).
13. A. M. Zhukov, "Mechanical properties of MA2 alloy in biaxial tension," *Izv. Akad. Nauk SSSR*, No. 9, 56–65 (1957).
14. A. S. Vavakin, R. A. Vasin, V. V. Viktorov, et al., "Proposals on the standardization of the submission of test results for publication in accordance with the All-Union State Standard 7.33–81 as applied to complex loading," *Izv. Akad. Nauk SSSR*, No. 6, 163–165 (1983).